Modified Volume-Delay Function Based on Traffic Fundamental Diagram: A Practical Calibration Framework for Estimating Congested and Uncongested Conditions

Yuyan "Annie" Pan[1]; Han Zheng, Ph.D.[2]; Jifu Guo, Ph.D.[3]; and Yanyan Chen, Ph.D.[4]

Abstract: Traffic congestion occurs when there is a mismatch between the demand for road use and the available capacity. The volume-delay function (VDF) can quantify the relationship between travel time and the volume of traffic on a particular link, and also provide insight into the state of a traffic system, such as whether it is congested or uncongested. In this paper, we present a VDF model that is based on the fundamental diagram and has two main components: (1) an improved VDF with fewer parameters that can handle both congested and uncongested traffic conditions, based on a fundamental diagram, and (2) a model-based VDF practical calibration framework for practical traffic applications that can determine key parameters for a link in a corridor. Our experiments using corridors in Los Angeles and Beijing demonstrate that our proposed analytical methods effectively calculate road impedance under congested conditions. The results indicate that the proposed model is superior to other existing models in terms of the root mean squared error (RMSE) and mean absolute error (MAE). In addition, our calibrated results indicate that the travel time index (TTI) in Los Angeles is 2.12, in Beijing is 1.74. The model proposed in this paper provides a useful calibration tool for enhancing model performance and improving the accuracy of travel time and speed estimates in traffic assignment. **DOI: 10.1061/JTEPBS.TEENG-7903.**

Author keywords: Bureau of public roads (BPR) function; Volume/capacity (V/C) ratio; Volume-delay functions (VDFs); Traffic congestion; Fundamental diagram.

Introduction

Motivation

Traffic assignment is a critical component of transportation planning, aimed at tackling current and future issues, including congestion, air pollution, and safety (Shefer 1994; Small and Gomez-Ibanez 1999; Armah et al. 2010; Gössling 2020). To achieve this, it is essential to strike a balance between the supply and demand of the traffic system, ensuring that road demand is met while enhancing transportation infrastructure capacity (Sheffi 1985; Omrani and Kattan 2012). Accurate estimation and calibration of the current traffic demand and supply are crucial in identifying and addressing congested or oversaturated conditions. Furthermore, effective traffic management (Ka et al. 2022) and congestion forewarning (Chen et al. 2022) can alleviate traffic congestion and improve mobility on roadways.

The four-step transportation planning process comprises trip generation, trip distribution, modal split, and traffic assignment. Traffic assignment analyzes link and path flow in a network by considering network topology, performance functions, origin-destination trip rates, and route choice behavior (Nie et al. 2004). The volume-delay function (VDF) is a critical component of traffic assignment, quantifying travel time caused by observed volume and road capacity (Kucharski and Drabicki 2017). VDF is essential for urban traffic planning, assignment, and control, and can accurately describe static urban traffic networks. VDF establishes the relationship between travel time, road traffic volume, and dynamic traffic state (Branston 1976; Nie and Zhang 2005; Patriksson 2015). Therefore, using an accurate VDF that captures network traffic flow characteristics and congestion state is crucial for effective traffic management and operation.

The study of VDF can be divided into two primary areas: parameter calibration and improvement of the traditional BPR function, which can lead to an enhanced BPR function. Alternatively, the calibration of existing VDF model parameters with measured data can help match local traffic flow. However, as traffic congestion worsens, there is a pressing need to investigate VDF under congested road conditions. Consequently, this study aims to integrate modified VDF with observation data to estimate traffic flow at the corridor level. This objective will be achieved in two ways: First, an improved VDF will be proposed for oversaturated conditions, based on the fundamental diagram. Secondly, the proposed VDF will be tested and validated in two cases in the Beijing and Los Angeles corridors by estimating congestion levels, speed, and other parameters.

The objective of the research in this paper is to tackle the limitations of the BPR function in dealing with traffic congestion. Furthermore, the proposed model in this study utilizes only one parameter, denoted as m, which is derived from the traffic flow model. This parameter, referred to as the maximum flow inertia

[1]Ph.D. Candidate, Beijing Key Laboratory of Traffic Engineering, Beijing Univ. of Technology, Beijing 100124, China. Email: yuyananniepan@gmail.com

[2]Lecturer, School of Traffic and Transportation, Beijing Jiaotong Univ., Beijing 100044, China. Email: hanzheng@bjtu.edu.cn

[3]Professor, Beijing Key Laboratory of Urban Transportation Operation Simulation and Decision Support, Beijing Transport Institute, Beijing 100000, China. Email: guojf@bjtrc.org.cn

[4]Professor, Beijing Key Laboratory of Traffic Engineering, Beijing Univ. of Technology, Beijing 100124, China (corresponding author). Email: cdyan@bjut.edu.cn

Note. This manuscript was submitted on January 9, 2023; approved on May 2, 2023; published online on September 14, 2023. Discussion period open until February 14, 2024; separate discussions must be submitted for individual papers. This paper is part of the ***Journal of Transportation Engineering, Part A: Systems***, © ASCE, ISSN 2473-2907.

coefficient, is introduced to regulate the smoothness or flatness of the curves for different planes across the range of feasible traffic congestion.

Objectives and Contributions

Despite numerous attempts to address the volume delay function calibration and estimation issue, there are still crucial challenges that require further investigation. First, the precision of model calibration outcomes needs to be enhanced, particularly in oversaturated conditions, to enable better estimation of traffic demand and efficient allocation of services for traffic assignment. Second, there is a lack of integration between the current model and the fundamental diagram. A comprehensive model calibration framework would provide practitioners and traffic planners with a complete set of application processes for transportation analysis and management.

In order to address this research gap, we propose a novel volume-delay function for traffic assignment that is based on the fundamental diagram and is able to effectively handle a wide range of traffic densities, including both congested and uncongested conditions. The main contributions of this study are summarized as follows:

- The proposed VDF, based on the fundamental diagram, accurately captures the traffic flow state during oversaturated conditions by integrating the traffic flow model into the volume delay function. This model requires fewer parameters to be calibrated than previous methods, yet it achieves a good fitting effect. Only one parameter, denoted as m, is necessary, which is derived from the macroscopic traffic flow model.
- We present a practical framework that utilizes fundamental diagrams to calibrate the key parameters of traffic flow and to test the effectiveness of our proposed VDF method. We also compare our model with existing VDF models and analyze the differences. Our findings indicate that our proposed model performs better than existing models in both the Los Angeles and Beijing cases, as measured by the root mean squared error (RMSE) and mean absolute error (MAE). Specifically, for Los Angeles, the RMSE and MAE values of our model are 3.44 and 2.13, respectively, while for Beijing, they are 3.54 and 2.13.
- We analyze the severity of congestion, speed, and the travel time index (TTI) using data typically collected in transportation studies. We then select two freeway corridor cases to conduct a more detailed analysis of our findings. Our calibrated results show that the TTI in Los Angeles is 2.12, whereas in Beijing, it is 1.74.

The remainder of this paper is organized as follows. Firstly, some related works are reviewed in "Literature Review." Secondly, in the "Methodology," this paper proposes the method framework of determining modified VDF based on the fundamental diagram. Next, "Case Study" implements the method using the Los Angeles I-405 corridor and Beijing corridor dataset and analyzes the determination results. Then, "Analysis of Results" analyze the estimation and calibration results of the selected two case. Finally, conclusions and discussion are included in "Conclusion."

Literature Review

Literature Review on Volume Delay Functions

The transportation planning field has proposed VDFs to evaluate the travel time performance of links. The Chicago Area Transportation Study (CATS) developed one of the first VDFs in the 1960s, expressed as an exponential function of the volume-to-capacity (V/C) ratio. Subsequently, other VDF-related functions were created, including the BPR function (BPR 1964), Davidson function (Davidson 1966, 1978), Akcelik function (Akcelik 1979, 1991), and conical function (Spiess 1990). In this section, we will review VDFs commonly used in traffic assignment studies.

Volume delay functions are used to determine travel time based on the V/C ratio at the link level. The parameters of a VDF include travel time, link volume, free-flow travel time, and practical capacity (Patriksson 2015). The BPR function, proposed by the US Bureau of Public Roads in 1964, is the most widely used VDF for analyzing the relationship between traffic volume and delays in transportation planning. It is computationally efficient, simple, and has good mathematical properties, requiring only two parameters (α and β) with standard reference values of 0.15 and 4, respectively (BPR 1964). However, it was developed based on highway observation traffic flow data, limiting its accuracy when applied to urban roads with different features such as intersections, bus lanes, stop signs, and signals (Skabardonis and Dowling 1997; Dowling et al. 1998). The BPR function also fails to accurately capture the dynamics of traffic flow (Pan et al. 2022) and queue evolution (Cheng et al. 2022; Zhou et al. 2022), and its accuracy decreases with higher values of β (Spiess 1990). Despite these limitations, the BPR function remains a popular choice for its simplicity and desirable mathematical properties.

Over the past forty years, researchers have studied the parameters and derivatives of the BPR function, and have developed alternative VDFs to address its limitations. Davidson (1966, 1978) proposed a modified VDF based on queuing theory that yields an infinite travel time when traffic volume reaches capacity. Akçelik (1979, 1991) developed a linear extension of Davidson's function and an alternative time-dependent form, which considers random delay and reasonable sensitivity for low and high V/C ratios. Tisato (1991) modified Davidson's model to address congestion duration during oversaturated conditions. Spiess (1990) proposed the conical function as an alternative to the BPR function, addressing its limitations. The conical function ensures unique link volumes and limits the steepness of the congestion curve to avoid issues with heavily congested links. Additionally, Spiess (1990) proposed seven conditions for "well-behaved" volume-delay functions to ensure increasing original form and first-order gradient and reasonable congestion effects when capacity is reached. The conical function outperforms the BPR function, and its transition is smooth because they share similar parameters. Recently, Zhou et al. (2022) revisited and improved on the standards of the conical function Spiess (1990) for a well-behaved congestion function, with a focus on queue-theoretical delay functions.

However, none of these static link travel time performance functions can approximate the overall queue evolution process. In order to bridge this gap, Newell (1982) and Cheng et al. (2022) proposed fluid-based polynomial arrival queue (PAQ) models, and Zhou et al. (2022) proposed a queue-based volume-delay function (QVDF) to describe the queue evolution process, with the inflow rate approximated by a polynomial function. Those methods open a new window to model and analyze dynamic traffic systems more efficiently and effectively.

The complexity of traffic flow makes it challenging to accurately determine its state. The existing VDFs have not adequately incorporated fundamental diagrams (FD), which establish the relationship between flow rate, speed, and density. FD divides the traffic flow into congested or uncongested conditions based on observed data. By incorporating FD, the resulting VDF can better conform to traffic flow characteristics and accurately differentiate between congested and uncongested states. To address this knowledge gap, this study introduces a modified VDF that incorporates FD calibration.

Literature Review on Modifying the V/C Ratio in VDF

The V/C ratio in the VDF represents the ratio of traffic volume per hour to the capacity of the corresponding link. It reflects both traffic demand (current traffic volume) and traffic supply (capacity) in the traffic system. When the value of V/C is less than 1, the relationship between speed and V/C reflects the undersaturated condition of the traffic flow on the road. When the V/C ratio is greater than 1, the traffic flow is in a congested state and the VDF reflects the traffic demand exceeding the road capacity, which cannot be directly measured. However, in the measured data, it is impossible to directly observe the case where V/C is greater than 1. This brings us to the definition of traffic demand. Traffic demand refers to the amount of vehicular or pedestrian traffic that is expected or experienced in a particular area or on a particular roadway. It is a measure of the need for transportation infrastructure, such as roads, highways, and public transit, and is an important consideration in transportation planning and management. Therefore, in traffic research, researchers can visualize the situation where V/C exceeds 1 (i.e., traffic demand is greater than road capacity), by using the measured data and the graph and mathematical fitting of V/C. Precise V/C ratio determination, especially in oversaturated situations or bottlenecks, is crucial for traffic assignment and planning.

Previous studies have explored estimating demand and V/C ratio in oversaturated conditions in the VDF. Small (1983) used a logit model of mode choice for work trips to estimate peak-period inflow demand resulting from queuing behind a single bottleneck with a constant capacity on urban highways. Moses et al. (2013) proposed the *symmetric* method to describe the relationship between road demand, travel time, and speed under oversaturated traffic. Florida Standard Urban Transportation Modeling Structure (FSUTMS) has adopted this method to improve travel forecasting and highway. Kucharski and Drabicki (2017) proposed the *quasi-density* method, which replaces the V/C ratio with k/k_c to estimate the relationship between road travel time and demand. This method improves VDF goodness-of-fit for hypercritical conditions. Huntsinger and Rouphail (2011) proposed the *demand-exceeds* method, which estimates demand for oversaturated signalized intersections and applies bottleneck and queue analysis to estimate demand beyond capacity for highways. They found that demand beyond capacity could be calculated by using the equation: *demand = capacity + queue length*. This method is useful for calculating time-dependent delay and estimating the influence area of the queue.

Previous literature has contributed significantly to understanding and modeling oversaturated traffic demand and flow. However, few studies have attempted to comprehensively handle oversaturated conditions and develop calibration frameworks based on identifying key parameters from freeway corridors, especially in cases with significant time delays. This paper addresses this gap by creating a basic traffic flow diagram and calibrating and estimating traffic flow parameters for various conditions, with a particular focus on oversaturated situations.

Methodology

Modified Volume-Delay Function Based on Fundamental Diagram

The traffic fundamental diagram is a valuable representation of the relationship among traffic flow, speed, and density for a specific section or corridor. This tool is crucial for comprehending traffic flow patterns and analyzing traffic behavior. Because the initial linear model suggested by Greenshields et al. (1935), numerous researchers have endeavored to devise more intricate models for describing traffic flow patterns. These models, such as those by Greenberg (1959), Drew (1964), Pipes (1967), Van Aerde (1995), Wang et al. (2011), and Ni et al. (2016), exhibit various strengths and characteristics. The S3 model is a streamlined approach to modeling speed-density relationships, using a simple S-shape function with just three parameters to capture light-traffic and jam conditions Cheng et al. (2021). Developed from the Butterworth filter, the function is derived through Laplace transforms and is both nonlinear and differentiable. The S3 model maintains consistency in modeling flow, speed, and density, and can be easily matched to available measurements of free-flow speed and maximum flow rates at critical density. Furthermore, the model provides an analytically derived speed-flow plane for analysis. The parameter m is introduced as the maximum flow inertia coefficient to control the smoothness or flatness of the curves for different planes across the feasible range of traffic congestion.

The general formula of the proposed S-shape model is expressed as

$$v = \frac{v_f}{[1 + (k/k_c)^m]^l} \tag{1}$$

where v_f is the free flow speed; k_c is the critical density that can result in a maximum traffic flow rate; and m and l are positive parameters to be determined. Considering the conservation law $q = kv$ and by multiplying both sides of Eq. (1) by the density k, we obtain the following low-density function:

$$q = \frac{k \cdot v_f}{[1 + (k/k_c)^m]^l} \tag{2}$$

As the flow function with respect to density is continuous, differentiating Eq. (2) leads to

$$\frac{dq}{dk} = \frac{v_f}{[1 + (k/k_c)^m]^l} - \frac{v_f \cdot l \cdot m \cdot \left(\frac{k}{k_c}\right)^m}{\left[1 + \left(\frac{k}{k_c}\right)^m\right]^{l+1}} = \frac{v_f}{\left[1 + \left(\frac{k}{k_c}\right)^m\right]^l} \cdot \left[1 - \frac{l \cdot m}{1 + (k_c/k)^m}\right] \tag{3}$$

At the point where the flow rates reach their maximum along the curve, the derivative of Eq. (3) at the critical density should equal zero, giving

$$\left.\frac{dq}{dk}\right|_{k=k_c} = 0 \Rightarrow \frac{v_f}{2^l} - v_f \cdot \frac{l \cdot m}{2^{l+1}} = 0 \Rightarrow l = \frac{2}{m} \tag{4}$$

Therefore, by substituting the relationship of $l = 2/m$ into Eqs. (1) and (2), the general form of the speed-density relationship and the maximum flow rates, when the density is at critical density, can be obtained as

$$v = \frac{v_f}{[1 + (k/k_c)^m]^{2/m}} \tag{5}$$

According to the conservation law of $q = kv$, we can obtain the flow-speed relationship function as

$$q = v \cdot k_c \cdot \left[\left(\frac{v_f}{v}\right)^{\frac{m}{2}} - 1\right]^{1/m} \tag{6}$$

Then, we also can capture the flow-density relationship function as

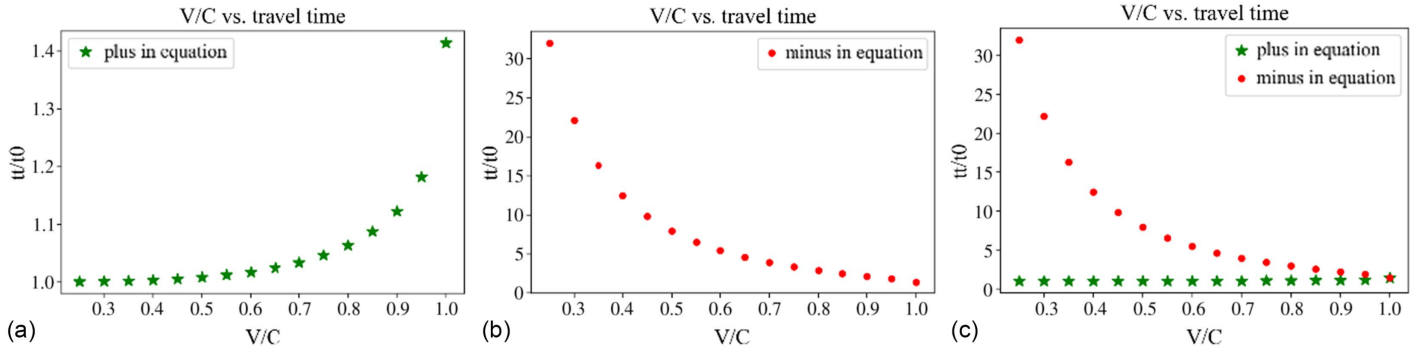

Fig. 1. Relationship between V/C and tt/t_0 in Eq. (18): (a) + in denominator; (b) − in denominator; and (c) integrated.

$$q = \frac{k \cdot v_f}{\left[1 + \left(\frac{k}{k_c}\right)^m\right]^{2/m}} \tag{7}$$

Further, when the density is the critical density k_c, we can obtain the maximum flow rates as

$$c = \frac{k_c \cdot v_f}{2^{2/m}} \tag{8}$$

Then, we can obtain the following by transposing the denominator:

$$4 \cdot c^m = k_c^m \cdot v_f^m \tag{9}$$

We assume the link length is L, and we can further derive

$$t_0 = \frac{L}{v_f} \tag{10}$$

$$t = \frac{L}{v} \tag{11}$$

By substituting Eqs. (10) and (11) into Eq. (9), we can obtain

$$q^m = 4c^m \cdot \left(\frac{t_0}{t}\right)^{\frac{m}{2}} - 4c^m \cdot \left(\frac{t_0}{t}\right)^m \tag{12}$$

Then, we can obtain the travel time function as shown in Eq. (13) by solving the quadratic equation

$$t = t_0 \cdot \left[\frac{2}{1 \pm \sqrt{1 - \left(\frac{q}{c}\right)^m}}\right]^{\frac{2}{m}} \tag{13}$$

The relationship between V/C and tt/t_0, described in Eq. (13), is visualized in Fig. 1(c), where the data is divided into two distinct parts. The asterisk point in Fig. 1(a) represent a positive correlation, showing that travel time increases with V/C. Meanwhile, the dot points in Fig. 1(b) indicate a negative correlation, demonstrating that travel time decreases with V/C. These positive and negative correlations are denoted by the "±" in the denominator of Eq. (13).

Further examination of Fig. 1 reveals that the inflection point occurs at $V/C = 1$. However, when V/C exceeds 1, Eq. (9) cannot accurately depict the relationship between demand and travel time, because observed volume data is always less than capacity. To remedy this, the symmetric method outlined in Section 2.2 is utilized to convert traffic flow when demand surpasses road capacity. As demonstrated in Fig. 2, the resulting model yields monotonically increasing nonlinear functions, ultimately summarized as a piecewise volume-delay function in Eq. (14).

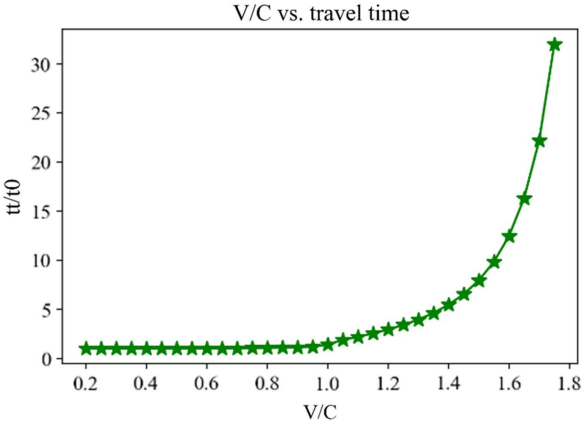

Fig. 2. Relationship between V/C and tt/t_0 in Eq. (14).

Further analysis of Fig. 1 shows that $V/C = 1$ is the inflection point. Eq. (13) is unable to reflect the relationship between demand and travel time when $V/C > 1$, because observed volume data is always less than capacity. To address this, the symmetric method described in Section 2.2 is used to convert the traffic flow when demand exceeds road capacity. As shown in Fig. 2, the final results of the proposed model are monotonically increasing nonlinear functions. These can be summarized as a piecewise volume-delay function, as shown in Eq. (14).

In summary, we could model the volume-delay function based on the fundamental diagram as

$$tt = \begin{cases} t_0 \cdot \left[\dfrac{2}{1 + \sqrt{1 - \left(\frac{V}{C}\right)^m}}\right]^{\frac{2}{m}}, & \text{if } V/C \le 1 \\ t_0 \cdot \left[\dfrac{2}{1 - \sqrt{1 - \left(2 - \frac{V}{C}\right)^m}}\right]^{\frac{2}{m}}, & \text{if } V/C > 1 \end{cases} \tag{14}$$

Model-Based Volume-Delay Function Practical Calibration Framework

Traffic data can be obtained from a variety of sources with different detection capabilities, including loop detectors, sensors, and GPS probe vehicles (Deng et al. 2013). Typically, volume or speed is used to model outputs that can be compared to empirical traffic data, which mainly consists of traffic counts and speeds.

Additionally, other empirical data, such as queue lengths, can be used as supplementary information to aid in the interpretation of model validation. During model validation, the proposed model outputs are compared to observed data, such as traffic flow and speed, to assess the quality of the model outputs (Chiu et al. 2011). Model calibration involves identifying a set of inputs and parameters that produce model outputs that are reasonably close to field observations (Wang et al. 2021). To evaluate the performance of the proposed model, various statistical tests, including linear regression analyses, can be used to quantify the goodness of fit between observed and estimated data. Evaluation indicators, such as RMSE, MAE, and R-squared (R^2), can be employed to assess the performance of the model (Willmott and Matsuura 2005).

The practical calibration framework proposed in this paper for the VDF utilizes a static traffic assignment system (Brederode et al. 2019). The framework, illustrated in Fig. 3, involves using a traffic flow model to determine the critical parameters of the segment, such as the free-flow speed (v_f), critical speed (v_c), critical density (k_c), and capacity (c). The traffic flow is then partitioned into congested and uncongested periods, based on the critical speed v_c. The key parameters are calibrated using the proposed VDF model and the observed data from various traffic periods. The proposed model outputs are then validated using measurement data and compared against observed data.

The input of this procedure is a combination of measurements q, k, v, with the output as the average travel time/speed for the segment.

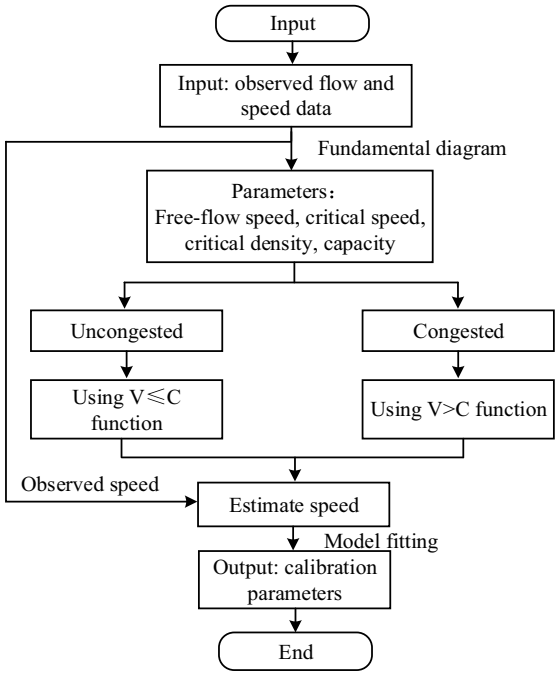

Fig. 3. Flowchart of the proposed VDF calibration framework.

Algorithm 1. Model-based VDF calibration framework

Input: Select observed traffic flow data for segments, i.e., speed v, flow q, and density k.

Output: Calibrated parameters v_f, v_c, k_c, c, α, β, J, and m, average travel time tt, and estimated speed $\hat{v}$.

Step 1: Using the traffic flow model to calibrate key parameters by measurement data, i.e., free-flow speed v_f, critical speed v_c, critical density k_c and capacity c.

Step 2: According to the derived critical speed v_c, distinguish the uncongested period and the congested period, e.g., the start time of congestion t_0, and end time of congestion t_3.

Step 3: In uncongested and congested periods, calculate the estimated average travel time and estimated speed respectively according to our proposed model.

Step 4: Use the observed data to calibrate parameters α, β, J, and m with the least square method.

Step 5: Analyze the results of various evaluation indicators between the observed values and the model estimates.

Case Study

Traffic Data Description

Case 1: Los Angeles Corridor

The I-405 corridor in Los Angeles was the data collection site for Case 1. On July 5, 2017, from 7:00 to 22:00, 11 detectors were installed along the corridor with absolute mileage ranging from 9.87 to 14.59, as illustrated in Fig. 4. The collected data included traffic flow, speed, and occupancy, which can be converted into density using Eq. (15) (May 1990). A contour map of the speed on the corridor (Fig. 5) showed the approximate congestion time and average duration at each detector, identifying Detector 3 as the bottleneck location. Detailed information on each detector can be found in Table 1

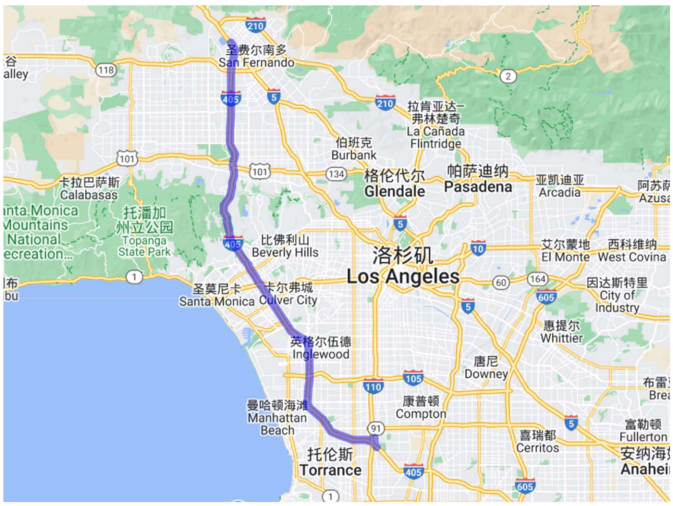

Fig. 4. Data acquisition in the Los Angeles corridor. (Map data © 2023 Google.)

$$k = \frac{5{,}280 \times \text{occ}}{l + d} \tag{15}$$

where occ is vehicle occupancy; l is the average vehicle length; and d is the detector area.

Case 2: Beijing Corridor

The West Third Ring corridor in Beijing, China was the data collection site for Case 2, as illustrated in Fig. 6. On June 8, 2018, from 6:00 to 12:00, 12 detectors were installed along the corridor. The collected data includes information on flow and speed. The traffic density can be calculated using the formula $q = kv$. A contour map of the speed on the corridor (Fig. 7) showed the approximate congestion time and average duration at each detector, identifying

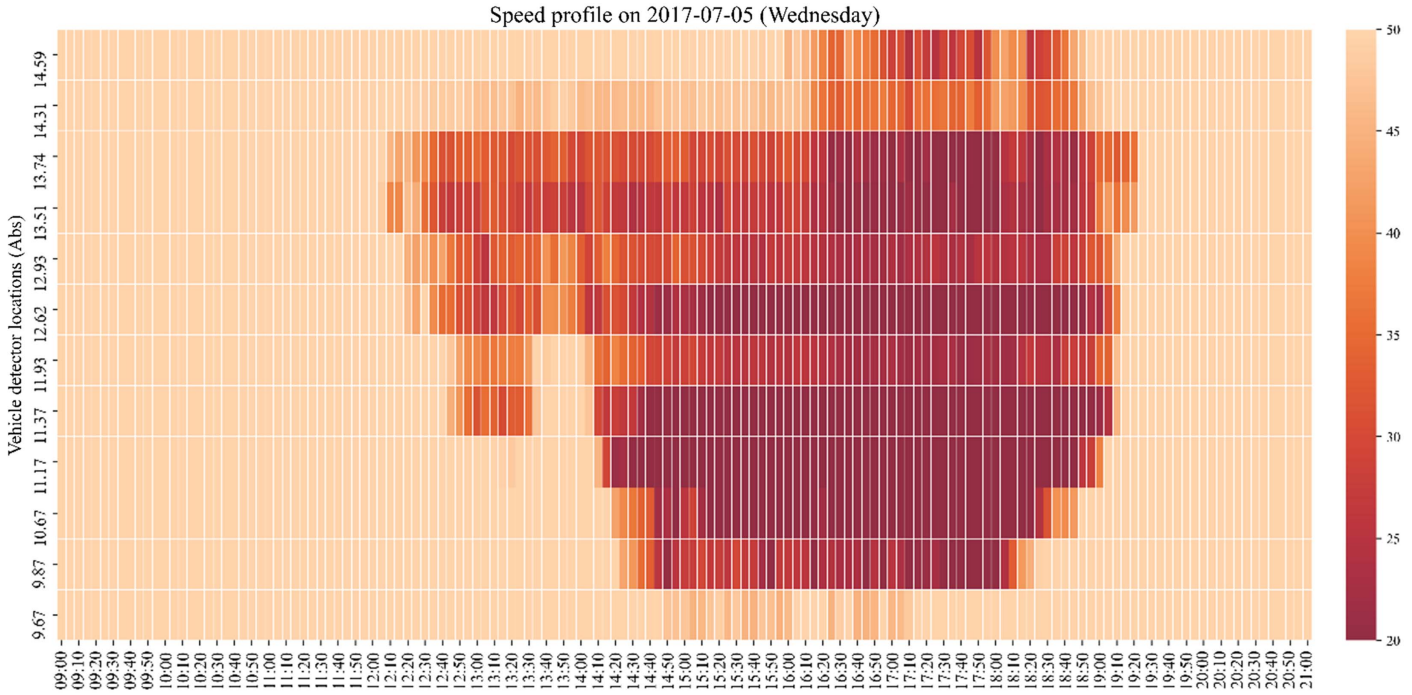

Fig. 5. Speed contour map of the Los Angeles corridor.

Table 1. Descriptive information of detectors in the Los Angeles corridor

Detector ID	Absolute mile	Length (mi)	Number of lanes
1	14.59	0.35	4
2	14.31	0.28	4
3	13.74	0.57	4
4	13.51	0.23	4
5	12.93	0.58	5
6	12.62	0.31	5
7	11.93	0.69	6
8	11.37	0.56	6
9	11.17	0.2	6
10	10.67	0.5	6
11	9.87	0.8	4

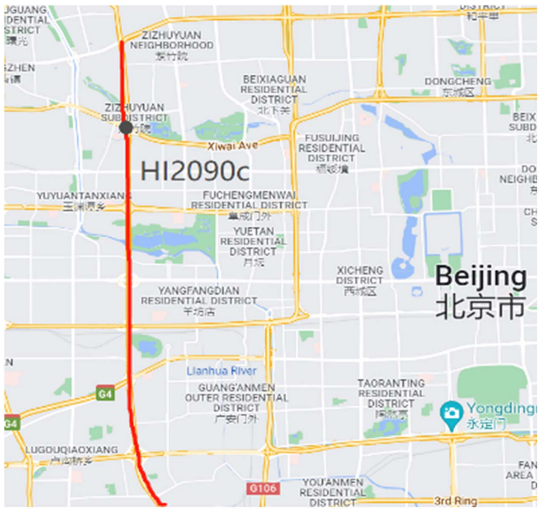

Fig. 6. Data acquisition in the Beijing corridor. (Map data © 2023 Google.)

HI2090c as the bottleneck location. Detailed information on each detector can be found in Table 2.

Identify Key Parameters and Duration in Bottlenecks

Fundamental diagrams for the Los Angeles case are shown in Fig. 8, which include the flow-speed, density-flow, and density-speed relationships. These relationships align with the fundamental characteristics of traffic flow, providing evidence of the reliability of the collected data. To calibrate the fundamental diagrams, the S3 model (Cheng et al. 2021) was used to fit the measurement data. The green dotted line in the figure represents the model-fitted results, while the red circles denote the observed traffic data.

The key parameters for each detector are shown in Table 3. The average free-flow speed v_f among all detectors is 70 mi/h. The critical speed v_c and critical density k_c show large variations, resulting in significant differences in capacity. The start and end times of congestion, as well as the duration and spatial extent of congestion, are illustrated in Fig. 9 using the space-time diagram. The red line represents the start of congestion; the blue line represents the end of congestion; and the yellow line represents the duration of congestion, P. Fig. 9 shows that the shape of congestion matches that shown in Fig. 7, indicating that the proposed method can effectively capture the congestion state of the bottleneck.

The calibrated fundamental diagram was further tested using the Beijing corridor, as shown in Fig. 10, which includes the flow-speed, density-flow, and density-speed relationships that conform to the essential traffic flow characteristics, affirming the reliability of the data. The S3 model was used to fit the measurement data and derive the fundamental diagrams, and the green dotted line represents the model-fitted results, while the red circles denote the observed traffic data. Key parameters for the bottleneck can be found in Table 4. Using the calibrated critical density, the traffic state can be divided into uncongested and oversaturated conditions, facilitating the use of Eq. (14) and the proposed calibration framework in Fig. 3 to estimate average travel time and speed.

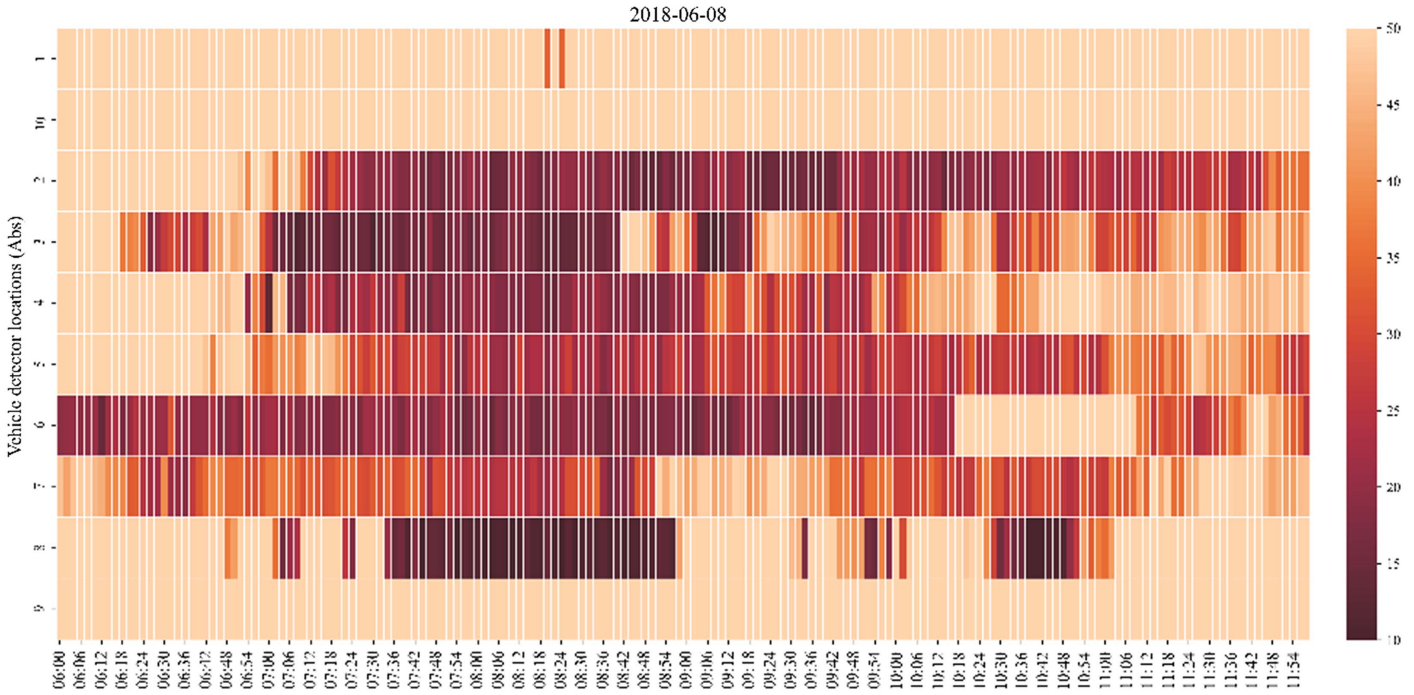

Fig. 7. Speed contour map of the Beijing corridor.

Table 2. Descriptive information of detectors in the Beijing corridor

Detector ID	Detector name	Length (m)	Number of lanes
1	HI2092c	500	2
2	HI2090c	1,653	3
3	HI8030c	1,093	3
4	HI2065c	924	3
5	HI2063c	777	3
6	HI8064c	512	3
7	HI8027c	1,157	3
8	HI8026c	587	3
9	HI8025c	746	3
10	HI8023c	333	3
11	HI8073c	148	3
12	HI8072c	613	3

Comparison of Different VDF Models

In this section, we assessed the congestion severity of the Los Angeles corridor using measured data and selected it for detailed analysis. We fitted four commonly-used VDFs: the BPR function, conical function, Akcelik function, and CATS function ($y = v_f \cdot 2^{V/C}$), to the dataset and optimized their parameters using the Solver function in Excel. Table 5 shows the model calibration results of the two cases. The VDFs accurately estimated the speed and V/C relationship of the selected links and provided insights into the model relationships between traffic volume and delays.

In the four VDFs considered in this study, all models except CATS performed well for the Los Angeles case. For the Beijing case, all R^2 values were greater than 0.95. The calibration results indicate that the BPR function, the conical function, and the function proposed in this paper are acceptable models for this corridor. However, graphically, the Akcelik and conical functions do not fit the observed data well, particularly the conical function, which is consistent with prior findings of Huntsinger and Rouphail (2011). Despite iterative parameter adjustment or optimization to minimize the sum-of-squared error, the conical model failed to accurately describe the observed data. The most significant finding of this study is the identification of a relatively simple approach for developing locally calibrated VDFs using freeway detector data, particularly in understanding demand beyond directly observable values when the volume equals capacity. This finding may prove beneficial to model developers.

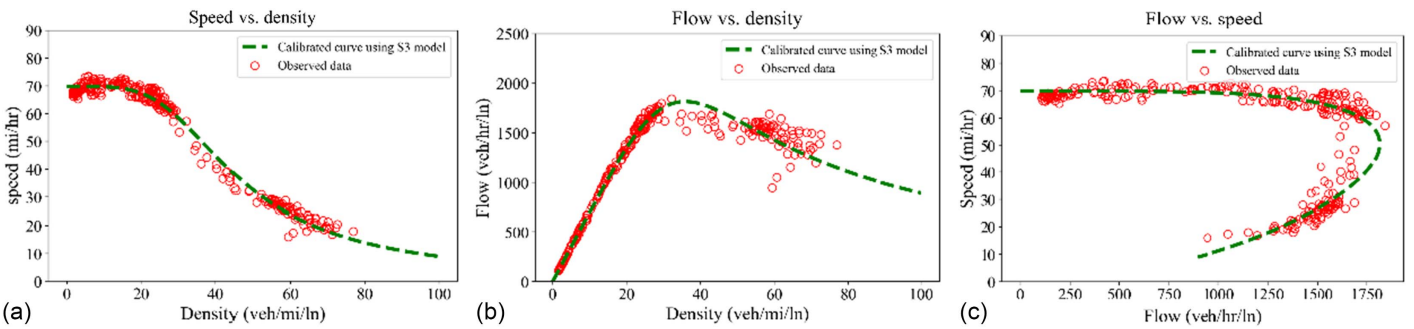

Fig. 8. Fundamental diagrams for the Los Angeles case: (a) density-speed relationship; (b) flow-density relationship; and (c) flow-speed relationship.

Table 3. Calibration results of key parameters in the Los Angeles case

Absolute mile	v_f (mi/h)	v_c (mi/h)	k_c (veh/mi/ ln)	c (veh/h/ ln)	t_0	t_3	P (min)
14.59	70	53.5	30.7	1,642	15:05	18:55	230
14.31	69.5	55	33.7	1,855	12:10	19:20	430
13.74	70	52	34.4	1,784	12:05	19:25	440
13.51	70	50.6	35.9	1,815	12:05	19:20	435
12.93	73	52.2	33.6	1,752	12:20	19:15	415
12.62	73	50.8	34.4	1,745	12:35	19:15	400
11.93	69	55.2	30.3	1,672	12:45	13:40	370
					13:55	19:10	
11.37	70.6	47.7	35.8	1,711	12:45	13:30	345
					14:10	19:10	
11.17	71.4	44	39.1	1,715	14:15	19:00	285
10.67	71.2	50	30	1,498	14:15	18:45	270
9.87	70.3	33.7	30	1,342	14:40	18:10	210

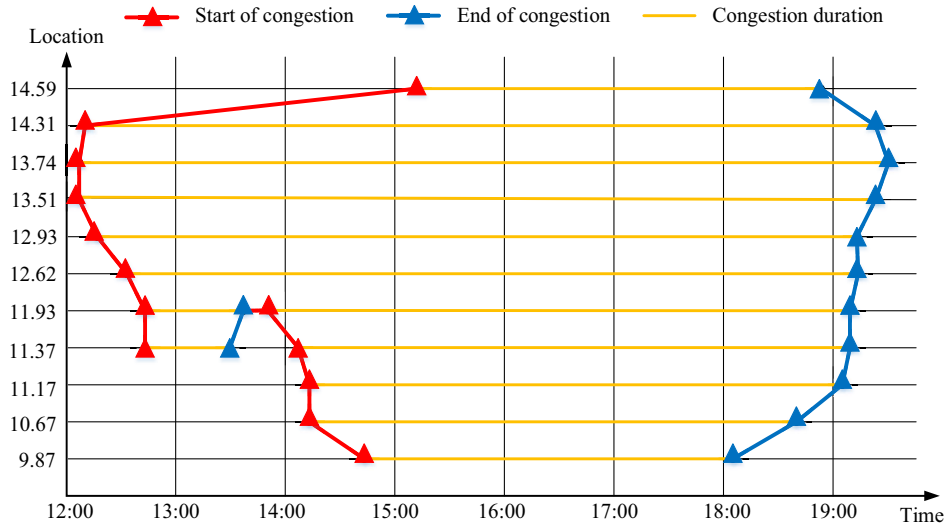

Fig. 9. Extent and duration of the bottleneck in time-space according to calibration results.

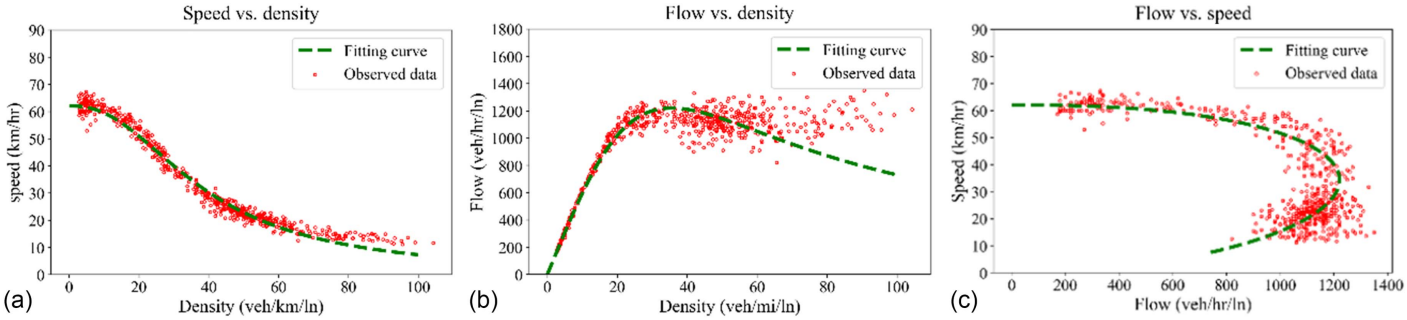

Fig. 10. Fundamental diagrams in the Beijing case: (a) density-speed relationship; (b) flow-density relationship; and (c) flow-speed relationship.

One of the key benefits of this research for model developers is the discovery of a straightforward method for developing locally calibrated VDFs using detector data from highways. This method requires only one parameter, m, which is derived from the fundamental diagram and represents the maximum flow inertia coefficient. The parameter m reflects the ability of a traffic system to maintain a full capacity state when the density deviates from the value of k_c; that is, the system's resistance to changes in density. This finding has implications for understanding demand beyond directly observable values when the volume is equal to capacity.

Table 4. Calibration results of key parameters in the Beijing case

v_f (km/h)	v_c (km/h)	k_c (veh/km/ ln)	c (veh/h/ ln)
62	34	36	1,220

Fig. 11(a) shows the relationship between the V/C ratio and speed across the different VDF models in Los Angeles case. Fig. 11(b) shows the relationship between the V/C ratio and speed across the different VDF models in Beijing case. The results in Table 5 demonstrate that the proposed VDF in this paper outperforms other classical models (BPR, conical, Akcelik, and CATS) in

Table 5. Comparison of model calibration results

Case	Function	Alpha	Beta	J	m	MAE	RMSE	R^2	When V = C tt/t_0	When V = 0 tt/t_0
Los Angeles	BPR	0.56	3.26	—	—	2.99	4.38	0.965	1.56	1
	Conical	4.79	1.20	—	—	5.22	6.79	0.967	2	0.95
	Akcelik	—	—	3,266	—	3.22	4.59	0.958	1.26	1
	CATS	—	—	—	—	9.07	11.55	0.838	2	1
	This paper	—	—	—	1.85	2.55	3.64	0.967	2.12	1
Beijing	BPR	0.81	2.16	—	—	2.27	2.83	0.983	1.81	1
	Conical	6.06	1.24	—	—	8.91	9.44	0.975	2	0.89
	Akcelik	—	—	7.29	—	2.38	2.85	0.983	0.67	1
	CATS	—	—	—	—	3.92	5.44	0.958	2	1
	This paper	—	—	—	1.12	2.13	2.78	0.983	3.45	1

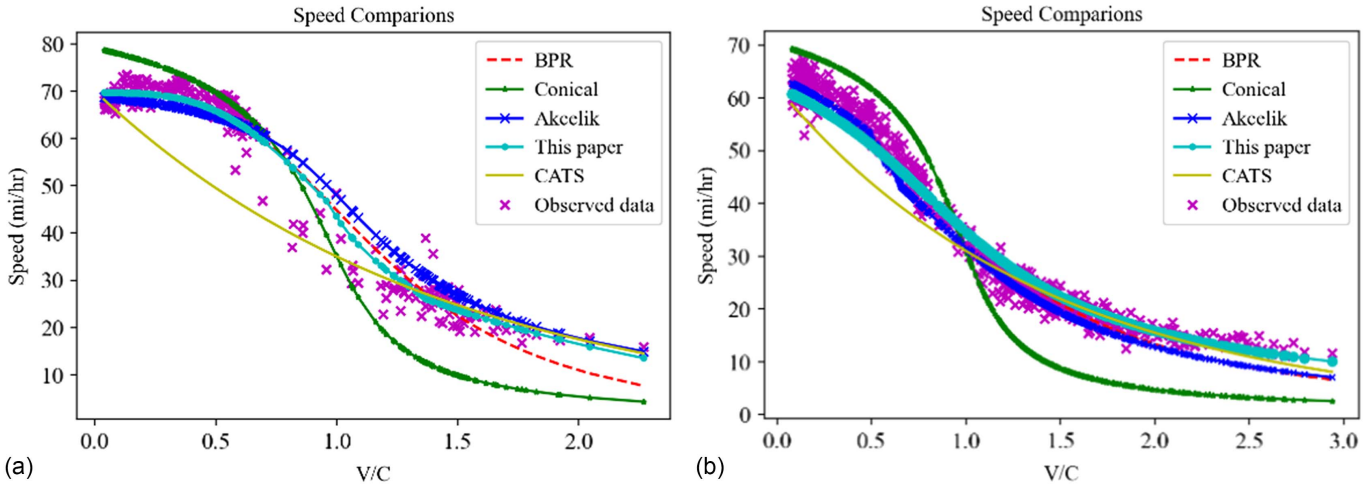

Fig. 11. Comparison of the relationship between V/C and speed of different models: (a) Los Angeles case; and (b) Beijing case.

terms of MAE, RMSE, and R^2. Specifically, the VDF achieves MAE, RMSE, and R^2 values of 2.55, 3.64, and 0.967 for the Los Angeles case and 2.13, 2.78, and 0.983 for the Beijing case, respectively. Moreover, the BPR function also shows favorable performance results. In addition, the results in Table 5 show the tt/t_0 ratio for the different VDF models when V = C and V = 0. For the Los Angeles case, when V/C = 1, the BPR function has an α value of 0.56 and a β value of 3.26, resulting in a tt/t_0 ratio of 1.56, indicating that the actual travel time is 1.56 times longer than the free-flow travel time when it is congestion. The conical and CATS functions have a tt/t_0 ratio of 2, while the Akcelik function and the function proposed in this paper have a ratio of 1.26 and 2.12, respectively. Combined with the results of RMSE, MAE, and R^2, it can be inferred that the method in this paper is more convincing when V = C, and the tt/t_0 ratio of 2.12 is more accurate. These results suggest that the proposed model has a greater effect on congestion estimation, especially in the case study of a bottleneck in the I-405 corridor with a maximum congestion time of over 400 min. When the observed flow in the link is zero, most of the functions have a tt/t_0 value of 1, with the exception of the conical function, which is close to 1.

Speed Estimation

Four different methods were used to fit the observed speed data from the two-corridor dataset: the symmetric method, quasi-density method, demand-exceeds method, and the method proposed in this study. We calculated the average travel time using the BPR function:

$$tt = t_0\left[1 + \alpha\left(\frac{V}{C}\right)^{\beta}\right] \tag{16}$$

where tt is travel time; t_0 is free-flow travel time; V is volume; C is capacity; and α, β are parameters.

Eq. (16) can be converted into a formula for calculating speed, as

$$v = \frac{v_f}{1 + \alpha \cdot \left(\frac{V}{C}\right)^{\beta}} \tag{17}$$

The estimated speed using the proposed model and other methods was compared by modifying the parameters to fit the observed speed data in the two-corridor dataset. According to Table 6, the proposed model is superior to other methods, with fewer calibrated parameters and lower error values, making it the optimal choice for accurately computing road impedance and reflecting traffic conditions. Fig. 12 depicts a time-dependent speed comparison between the estimated and measured speeds for the Los Angeles case, while Fig. 13 shows the estimated and observed speed for the bottleneck

Table 6. Calibrated parameters and sensitivity analysis using the different methods in the Los Angeles case

Method	Alpha	Beta	m	RMSE	MAE
Symmetric	0.33	10.38	—	3.88	2.93
Quasi-density	0.62	3.07	—	3.53	2.66
Demand-exceeds	0.33	20.48	—	3.53	2.47
This paper	—	—	1.85	3.44	2.13

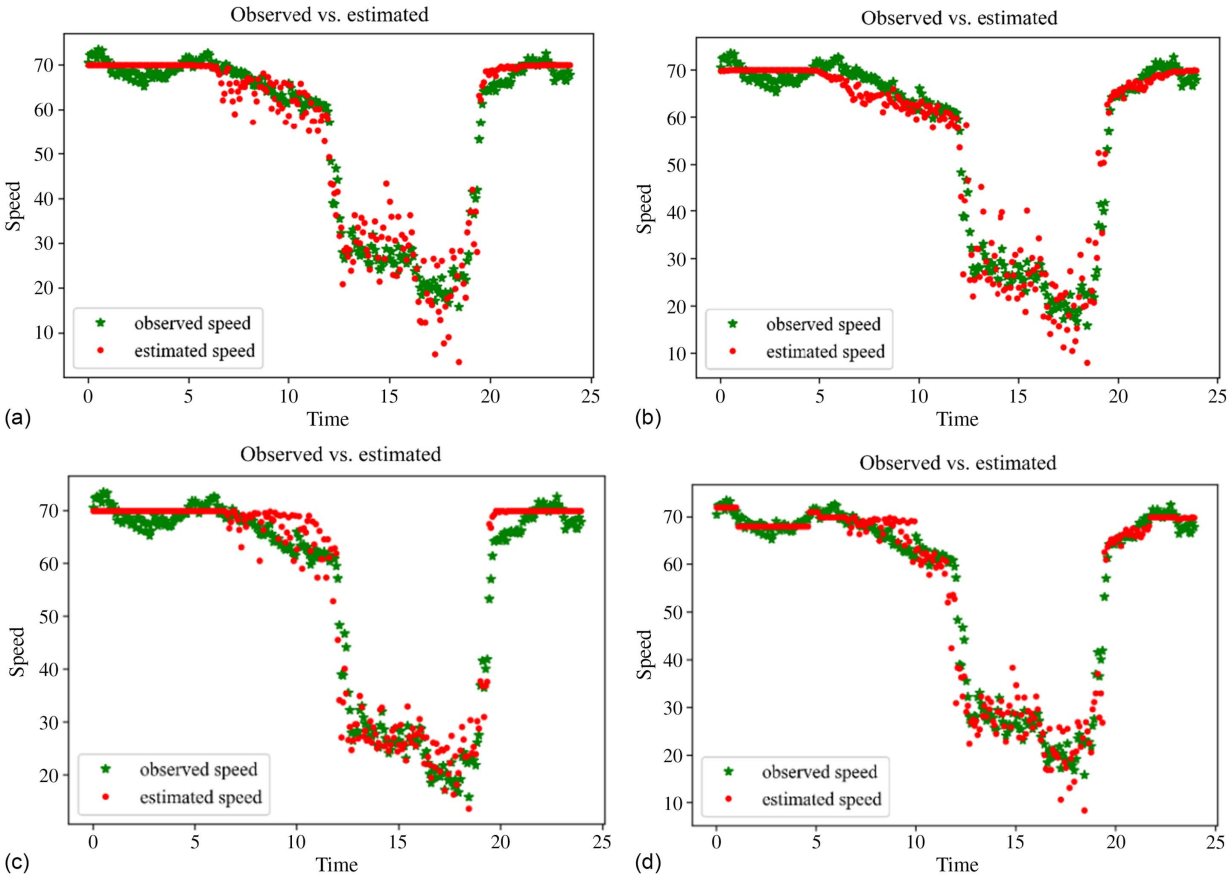

Fig. 12. Comparison between time-dependent observed and estimated speed using different methods in the Los Angeles case: (a) symmetric method; (b) quasi-density method; (c) demand-exceeds method; and (d) this paper method.

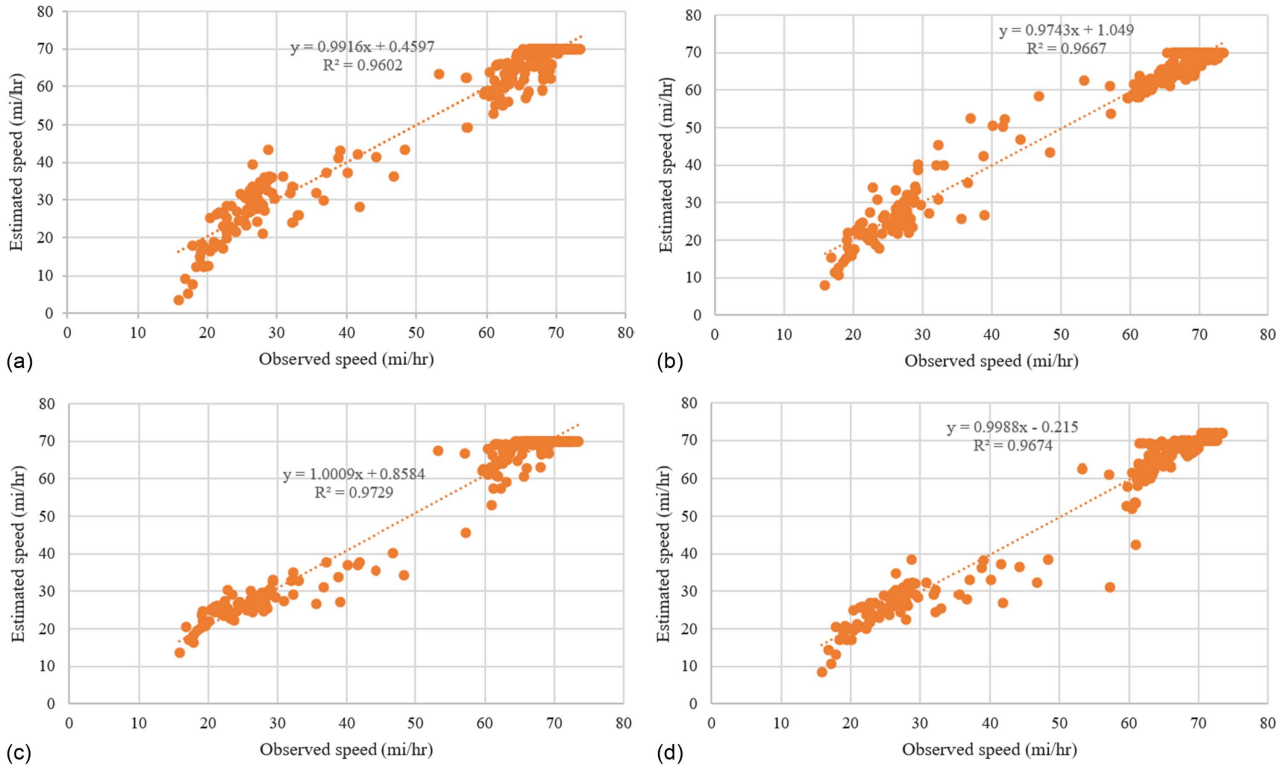

Fig. 13. Comparison between observed and estimated speed using different methods in the Los Angeles case: (a) symmetric method; (b) quasi-density method; (c) demand-exceeds method; and (d) this paper's method.

Table 7. Calibrated parameters and sensitivity analysis using the different methods in the Beijing case

Method	Alpha	Beta	m	RMSE	MAE
Symmetric	2.03	3.88	—	7.99	5.04
Quasi-density	0.81	2.23	—	3.56	2.99
Demand-exceeds	1.35	2.97	—	6.91	5.33
This paper	—	—	2.5	3.54	2.13

throughout the analysis period. The proposed model performed exceptionally well, with an R^2 value of 0.9674, and had a slight advantage over other methods in terms of RMSE, MAE, and R^2, as demonstrated in Table 6 and Figs. 12 and 13. These findings suggest that the proposed model is a suitable and reliable approach for estimating road impedance and accurately reflecting the traffic system.

To evaluate the effectiveness of our proposed framework, we tested it using the Beijing corridor dataset and analyzed the calibrated parameters and sensitivity using various methods, which are presented in Table 7. Furthermore, Fig. 14 displays a comparison of the observed and estimated time-dependent speeds, while Fig. 15 illustrates the estimated and observed speeds throughout the analysis period for the bottleneck. The estimated speeds closely matched the observed values, with an R^2 value of 0.9726 by the proposed model presented in this paper. The results demonstrated an excellent fit to all estimated values, with the approach in this paper having a slight advantage over other methods in terms of RMSE, MAE, and R^2, as depicted in Table 7 and Figs. 14 and 15.

Analysis of Results

The TTI is the ratio of the travel time during the peak period to the time required to make the same trip at free-flow speeds (Pu 2011). Free-flow travel time refers to the time required for a vehicle to travel on a road segment with low traffic volume and good road conditions, while actual travel time refers to the time required for a vehicle to travel on a road segment with actual traffic volume and congested road conditions. Therefore, the higher the TTI of a road segment, the higher the level of traffic congestion, and the longer the travel time required for vehicles relative to free-flow conditions. TTI is commonly used to measure the level of traffic congestion and is often used in transportation planning and management.

Further analysis of the calibration results shows that, for the BPR function, when $\alpha = 0.15$, $\beta = 4$, the actual travel time of a unit section is 1.15 times longer than the free flow travel time, indicating that when the road reaches saturation under the recommended parameters of the US Federal Highway Administration, the actual travel time of a unit section is 1.15 times that of the free-flow travel time. For the proposed VDF function in Eq. (14), in the Los Angeles case, when $V/C = 1$ and $m = 1.85$, the tt/t_0 is 2.12 according to the fitted model based on the measured data. In the Beijing case, when $V/C = 1$ and $m = 2.5$, the tt/t_0 is 1.74. Therefore, the TTI in the Los Angeles case is 2.12, while in the Beijing case it is 1.74.

Upon comparing the Los Angeles and Beijing case studies, it is evident that the TTI in Los Angeles is higher than that of Beijing, indicating longer delay times and sustained congestion per unit section. Moreover, Tables 3 and 4 show that the bottleneck's

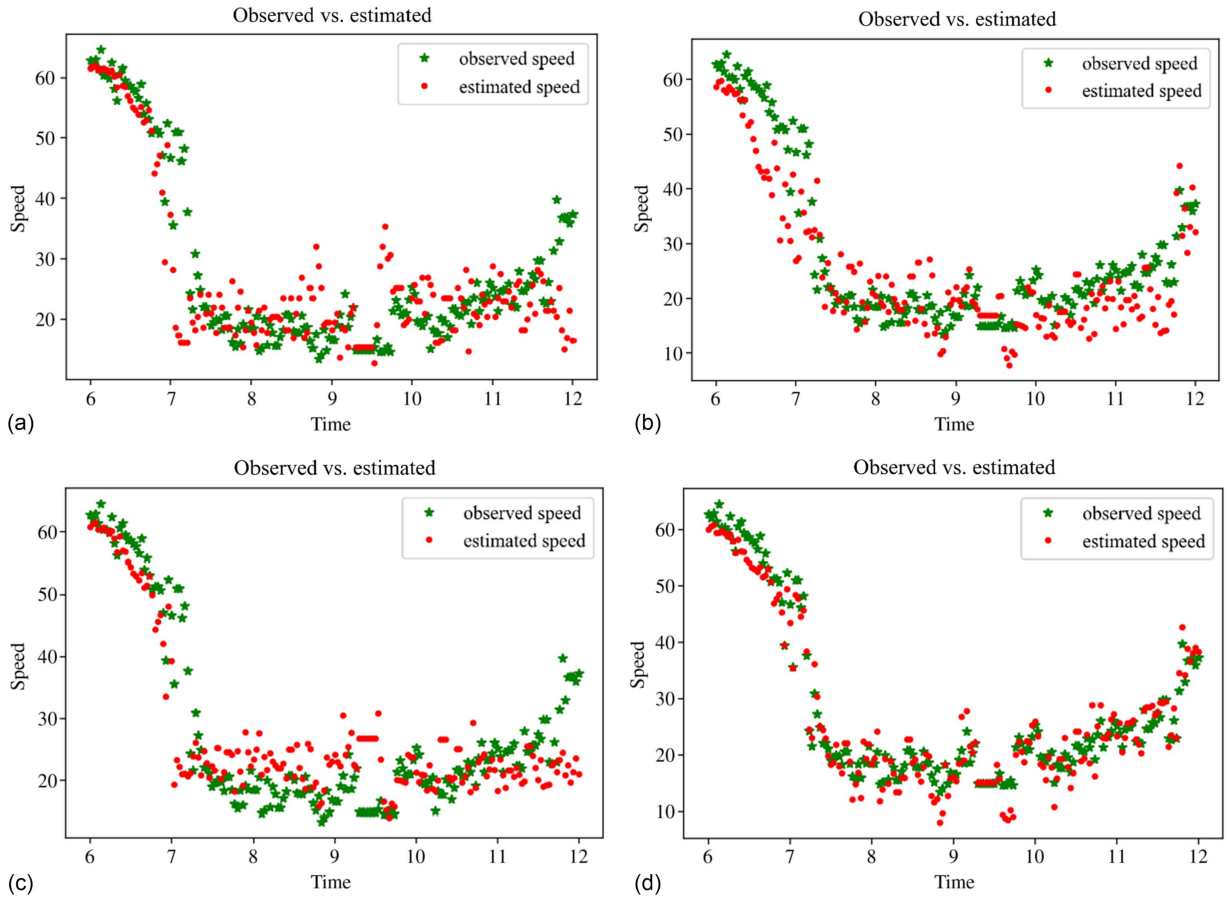

Fig. 14. Comparison between time-dependent observed and estimated speed using different methods in the Beijing case: (a) symmetric method; (b) quasi-density method; (c) demand-exceeds method; and (d) this paper's method.

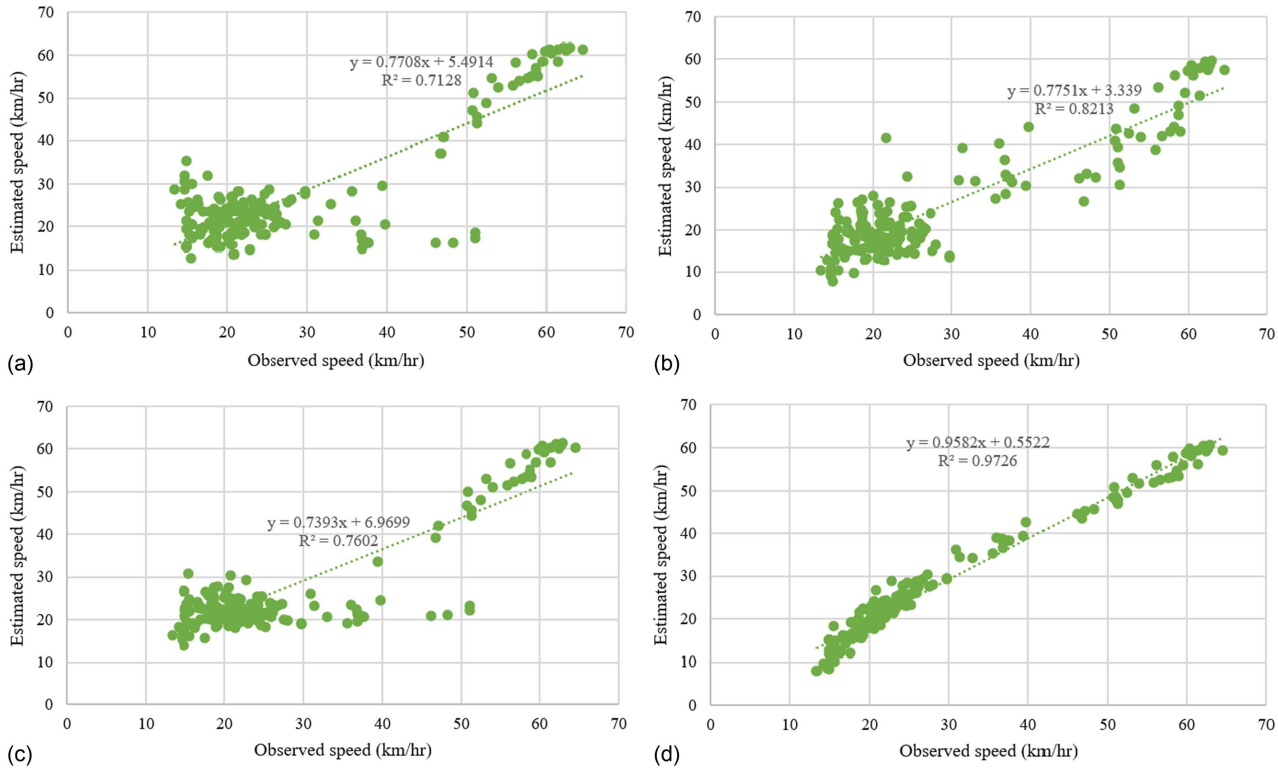

Fig. 15. Comparison between observed and estimated speed using different methods in the Beijing case: (a) symmetric method; (b) quasi-density method; (c) demand-exceeds method; and (d) this paper's method.

free-flow speed in Los Angeles is 70 mi/h, the critical speed is 52 mi/h, and the actual traffic capacity is 1,784 vehicles per hour per lane, while for Beijing, the values are 62 km/h, 34 km/h, and 1,220 vehicles per hour per lane, respectively. The critical parameters in Los Angeles, including free-flow speed, critical speed, and actual traffic capacity, are all higher than in Beijing, suggesting greater traffic flow and faster travel speed in Los Angeles.

Conclusion

The VDF plays an essential role in traffic assignment and traffic network analysis. This paper proposes an improved VDF based on the fundamental diagram and verifies the model based on the measured data in a corridor. The proposed model has great applicability and accuracy, which can be used as a reference for traffic demand analysis and macro model establishment for all traffic conditions. The main contributions are as follows:

- Using the fundamental diagram model as a basis, we derived an enhanced VDF formula to calculate the relationship between road section flow and travel time under congested traffic conditions. Our findings demonstrate that this method accurately reflects the actual traffic flow operations, resulting in smaller errors in speed estimation compared to models tested in the literature. In both cases, the RMSE and MAE values were lower than those reported in previous studies.
- The model produces a travel time index for the Los Angeles and Beijing cases, which is the ratio of the average travel time to free flow time. The Los Angeles case had a travel time index of 2.12, while the Beijing case had a travel time index of 1.74. A higher travel time index implies a greater degree of traffic congestion on a road section. Therefore, the Los Angeles case has longer delays and more prolonged average congestion times per section than the Beijing case, as indicated by its higher travel time index.
- A practical calibration framework for obtaining crucial parameters in traffic systems was developed by using a volume-delay function. The proposed method simplifies practical engineering applications by requiring adjustment of only one unknown parameter. Furthermore, it combines the traffic flow model with the VDF to capture traffic flow behavior from different perspectives, particularly in supersaturated traffic congestion systems. The proposed method accurately calculates road impedance in such systems, providing a reliable basis for traffic allocation.
- The proposed method has several advantages that make it well-suited for practical traffic planning. One key advantage is that it requires fewer parameters to be calibrated, making it easier to apply in real-world situations. Additionally, the method combines a traffic flow model with the VDF, which allows for a more comprehensive understanding of traffic flow characteristics across multiple resolutions, particularly during periods of congestion.

Future research could explore the use of this method in more complex scenarios that involve nonrecurring delays, such as those caused by weather, accidents, or construction projects.

Data Availability Statement

The data used to support the findings of this study are available from the corresponding author upon request.

Acknowledgments

The authors received no financial support for the research, authorship, and/or publication of this article.

Author contributions: Study conception and design: Yuyan (Annie) Pan and Han Zheng; data collection: Yuyan (Annie) Pan; analysis and interpretation of results: Yuyan (Annie) Pan; and draft manuscript preparation: Yuyan (Annie) Pan, Han Zheng, Jifu Guo, and Yanyan Chen. All authors reviewed the results and approved the final version of the manuscript.

References

Akcelik, R. 1979. "A graphical explanation of the two principles and two techniques of traffic assignment." *Transp. Res. A: Policy Pract.* 13 (3): 179–184.

Akçelik, R. 1991. "Travel time functions for transport planning purposes: Davidson's function, its time dependent form and alternative travel time function." *Aust. Road Res.* 21 (3): 1–13.

Armah, F. A., D. O. Yawson, and A. A. Pappoe. 2010. "A systems dynamics approach to explore traffic congestion and air pollution link in the city of Accra, Ghana." *Sustainability* 2 (1): 252–265. https://doi.org/10.3390/su2010252.

BPR (Bureau of Public Roads). 1964. *Traffic assignment manual*. Washington, DC: Urban Planning Division, US Department of Commerce.

Branston, D. 1976. "Link capacity functions: A review." *Transp. Res.* 10 (4): 223–236. https://doi.org/10.1016/0041-1647(76)90055-1.

Brederode, L., A. Pel, L. Wismans, E. de Romph, and S. Hoogendoorn. 2019. "Static traffic assignment with queuing: Model properties and applications." *Transportmetrica A: Transport Sci.* 15 (2): 179–214. https://doi.org/10.1080/23249935.2018.1453561.

Chen, Y., S. Li, Y. Pan, and J. Zhang. 2022. "Urban expressway congestion forewarning based on slope change of traffic flow fundamental diagram." *J. Transp. Eng. Part A Syst.* 148 (6): 04022030. https://doi.org/10.1061/JTEPBS.0000687.

Cheng, Q., Z. Liu, J. Guo, X. Wu, R. Pendyala, B. Belezamo, and X. S. Zhou. 2022. "Estimating key traffic state parameters through parsimonious spatial queue models." *Transp. Res. Part C Emerging Technol.* 137 (Apr): 103596. https://doi.org/10.1016/j.trc.2022.103596.

Cheng, Q., Z. Liu, Y. Lin, and X. Zhou. 2021. "An S-shaped three-parameter (S3) traffic stream model with consistent car following relationship." *Transp. Res. Part B Methodol.* 153 (Nov): 246–271. https://doi.org/10.1016/j.trb.2021.09.004.

Chiu, Y. C., J. Bottom, M. Mahut, A. Paz, R. Balakrishna, T. Waller, and J. Hicks. 2011. *Dynamic traffic assignment: A primer*. Transportation Research Circular E-C153. Washington, DC: Transportation Research Board.

Davidson, K. B. 1966. "A flow travel time relationship for use in transportation planning." In Vol. 3 of *Proc., Australian Road Research Board Conf.* Port Melbourne, VIC, Australia: Australian Road Research Board.

Davidson, K. B. 1978. "The theoretical basis of a flow-travel time relationship for use in transportation planning." *Aust. Road Res.* 8 (1): 32–35.

Deng, W., H. Lei, and X. Zhou. 2013. "Traffic state estimation and uncertainty quantification based on heterogeneous data sources: A three detector approach." *Transp. Res. Part B Methodol.* 57 (Nov): 132–157. https://doi.org/10.1016/j.trb.2013.08.015.

Dowling, R. G., R. Singh, and W. Wei-Kuo Cheng. 1998. "Accuracy and performance of improved speed-flow curves." *Transp. Res. Rec.* 1646 (1): 9–17. https://doi.org/10.3141/1646-02.

Drew, D. R. 1964. *Theoretical approaches to the study and control of freeway congestion*. College Station, TX: Texas Transportation Institute.

Gössling, S. 2020. "Integrating e-scooters in urban transportation: Problems, policies, and the prospect of system change." *Transp. Res. Part D Transp. Environ.* 79 (Feb): 102230. https://doi.org/10.1016/j.trd.2020.102230.

Greenberg, H. 1959. "An analysis of traffic flow." *Oper. Res.* 7 (1): 79–85. https://doi.org/10.1287/opre.7.1.79.

Greenshields, B. D., J. R. Bibbins, W. S. Channing, and H. H. Miller. 1935. "A study of traffic capacity." In Vol. 14 of *Proc., Highway Research Board*. Washington, DC: National Research Council, Highway Research Board.

Huntsinger, L. F., and N. M. Rouphail. 2011. "Bottleneck and queuing analysis: Calibrating volume-delay functions of travel demand models." *Transp. Res. Rec.* 2255 (1): 117–124. https://doi.org/10.3141/2255-13.

Ka, E., S. Sharma, and S. Ukkusuri. 2022. "Leveraging location-based data for assessing network-level traffic impact of lane management: A case study of Alex Fraser Bridge." *J. Transp. Eng. Part A Syst.* 148 (12): 04022105. https://doi.org/10.1061/JTEPBS.0000760.

Kucharski, R., and A. Drabicki. 2017. "Estimating macroscopic volume delay functions with the traffic density derived from measured speeds and flows." *J. Adv. Transp.* 2017 (Jan): 4629792. https://doi.org/10.1155/2017/4629792.

May, A. D. 1990. *Traffic flow fundamentals*. Englewood Cliffs, NJ: Prentice-Hall.

Moses, R., E. Mtoi, S. Ruegg, H. McBean, and P. Brinckerhoff. 2013. *Development of speed models for improving travel forecasting and highway performance evaluation*. Rep. No. BDK83-977-14. Tallahassee, FL: DOT.

Newell, G. F. 1982. *Applications of queueing theory*. 2nd ed. New York: Chapman and Hall.

Ni, D., J. D. Leonard, C. Jia, and J. Wang. 2016. "Vehicle longitudinal control and traffic stream modeling." *Transp. Sci.* 50 (3): 1016–1031. https://doi.org/10.1287/trsc.2015.0614.

Nie, X., and H. M. Zhang. 2005. "Delay-function-based link models: Their properties and computational issues." *Transp. Res. Part B Methodol.* 39 (8): 729–751. https://doi.org/10.1016/j.trb.2004.10.002.

Nie, Y., H. M. Zhang, and D. H. Lee. 2004. "Models and algorithms for the traffic assignment problem with link capacity constraints." *Transp. Res. Part B Methodol.* 38 (4): 285–312. https://doi.org/10.1016/S0191-2615(03)00010-9.

Omrani, R., and L. Kattan. 2012. "Demand and supply calibration of dynamic traffic assignment models: Past efforts and future challenges." *Transp. Res. Rec.* 2283 (1): 100–112. https://doi.org/10.3141/2283-11.

Pan, Y., J. Guo, and Y. Chen. 2022. "Calibration of dynamic volume-delay functions: A rolling horizon-based parsimonious modeling perspective." *Transp. Res. Rec.* 2676 (2): 606–620. https://doi.org/10.1177/03611981211044727.

Patriksson, M. 2015. *The traffic assignment problem: Models and methods*. Mineola, NY: Courier Dover Publications.

Pipes, L. A. 1967. "Car following models and the fundamental diagram of road traffic." *Transp. Res.* 1 (1): 21–29. https://doi.org/10.1016/0041-1647(67)90092-5.

Pu, W. 2011. "Analytic relationships between travel time reliability measures." *Transp. Res. Rec.* 2254 (1): 122–130. https://doi.org/10.3141/2254-13.

Shefer, D. 1994. "Congestion, air pollution, and road fatalities in urban areas." *Accid. Anal. Prev.* 26 (4): 501–509. https://doi.org/10.1016/0001-4575(94)90041-8.

Sheffi, Y. 1985. Vol. 6 of *Urban transportation networks: Equilibrium analysis with mathematical programming methods*. Englewood Cliffs, NJ: Prentice-Hall.

Skabardonis, A., and R. Dowling. 1997. "Improved speed-flow relationships for planning applications." *Transp. Res. Rec.* 1572 (1): 18–23. https://doi.org/10.3141/1572-03.

Small, K. A. 1983. "The incidence of congestion tolls on urban highways." *J. Urban Econ.* 13 (1): 90–111. https://doi.org/10.1016/0094-1190(83)90047-5.

Small, K. A., and J. A. Gomez-Ibanez. 1999. "Urban transportation." In Vol. 3 of *Handbook of regional and urban economics*, 1937–1999. Amsterdam, Netherlands: Elsevier.

Spiess, H. 1990. "Conical volume-delay functions." *Transp. Sci.* 24 (2): 153–158. https://doi.org/10.1287/trsc.24.2.153.

Tisato, P. 1991. "Suggestions for an improved Davidson travel time function." *Aust. Road Res.* 21 (2): 85–100.

Van Aerde, M. 1995. "Single regime speed-flow-density relationship for congested and uncongested highways." In Vol. 6 of *Proc., 74th Annual*

Conference of the Transportation Research Board. Washington, DC: Transportation Research Board.

Wang, H., J. Li, Q. Y. Chen, and D. Ni. 2011. "Logistic modeling of the equilibrium speed-density relationship." *Transp. Res. Part A Policy Pract.* 45 (6): 554–566. https://doi.org/10.1016/j.tra.2011.03.010.

Wang, S., X. Chen, and X. Qu. 2021. "Model on empirically calibrating stochastic traffic flow fundamental diagram." *Commun. Transp. Res.* 1 (Dec): 100015. https://doi.org/10.1016/j.commtr.2021.100015.

Willmott, C. J., and K. Matsuura. 2005. "Advantages of the mean absolute error (MAE) over the root mean square error (RMSE) in assessing average model performance." *Clim. Res.* 30 (1): 79–82. https://doi.org/10.3354/cr030079.

Zhou, X. S., Q. Cheng, X. Wu, P. Li, B. Belezamo, J. Lu, and M. Abbasi. 2022. "A meso-to-macro cross-resolution performance approach for connecting polynomial arrival queue model to volume-delay function with inflow demand-to-capacity ratio." *Multimodal Transp.* 1 (2): 100017. https://doi.org/10.1016/j.multra.2022.100017.